

A Design Methodology
for
Zero Reaction Robots

Evangelos Papadopoulos

Assistant Professor

Department of Mechanical Engineering and

Centre for Intelligent Machines

McGill University

Montreal, PQ H3A 2A7

Ahmed Abu-Abed

Electrical Distribution and Control Division

General Electric Canada

Mississauga, ON L5N 5P9

Submitted as a Contribution to the
Special Forum '94 Issue of the CSME Transactions

ABSTRACT

In many applications of advanced robotic systems, reaction forces and moments transmitted by a manipulator to its base are highly undesirable. Such reactions reduce the accuracy of high-speed manipulators, destroy zero-g environments in space, require the use of thruster fuel to stabilize free-flying space robots, or excite suspension modes in mobile robotic systems. In this paper, we analyze the problem of force and torque transmission in robotic systems, and propose design and planning methods that can reduce it, or eliminate it. It is shown that designing a force-balanced manipulator with an invariant mass matrix, and employing appropriate trajectory planning, can result in reactionless motions. Two redundant planar manipulator designs demonstrate the usefulness of the proposed methods. An important advantage of these methods is that manipulators can be used either as redundant ones, or as two DOF reactionless systems.

I. INTRODUCTION

In many applications of advanced robotic systems, reaction forces transmitted by a manipulator to its base are highly undesirable. In an industrial setting, the accuracy of a rapidly accelerating manipulator will be degraded by vibrations induced by the transmission of large reaction forces to its mounts, [1]. In space, dynamic forces due to the accelerating links of a manipulator mounted on a satellite will disturb the position and orientation of the latter [2,3]. If allowed to transmit reaction forces, manipulators operating in a micro-gravity environment will have adverse effects on it [4]. Manipulators mounted on compliant mobile bases, be it a truck, a Mars rover, or the Shuttle Canadarm, will inevitably excite the base dynamics and result in poor dynamic performance and accuracy [5,6].

Moving a manipulator slowly is the simplest way to reduce the reactions to within acceptable levels. Reducing manipulator reactions by cost function minimization applied to redundant manipulators was proposed in [7]. Complete shaking force elimination can be achieved by fixing the center of gravity of the manipulator; this is accomplished by the addition of counterweights

or by relocating the support point of the manipulator [1,8,9,10,11]. Minimization of the rocking moment can be accomplished by introducing counteracting torques. This is normally done using additional actuators with a preset inertia, along with a suitable controller [1]. However, these actuators can not be used to enhance the system manipulative capabilities. In space, there exist paths that if followed by a manipulator mounted on a free-floating spacecraft, they will result in zero attitude (orientation) disturbance for the spacecraft. However, use of such paths may require relocating the spacecraft to some favorable initial position [5]. In addition, they will not eliminate reaction forces, i.e. the spacecraft will still translate.

In this paper we analyze the problem of force and moment transmission by manipulators and propose guidelines that can result in reactionless motions. These include static balancing of the manipulator, invariance of its mass matrix, and use of special joint-space reactionless trajectories. Two planar three Degree-of-Freedom (DOF) manipulators with two or three direct drive actuators mounted at their base and sharing a common axis are employed. The system Center of Mass (CM) is fixed by static balancing, and the dynamics of the system are rendered invariant. The latter feature simplifies the planning of reactionless paths, by requiring that such paths belong in fixed orientation joint space planes. Motions planned in such a way result in minimal reactions, whereas non-reactionless motions are shown to transmit large moments and forces. An advantage of these designs is that the manipulators can be used either for tasks that require three Degrees-of-Freedom (DOF), or as two DOF reactionless systems.

II. BASE FORCE AND MOMENT BALANCING

Consider a manipulator as an articulated mechanism that applies a force \mathbf{f}_B and a moment \mathbf{n}_B to its base, see Fig. 1. In the presence of gravity, the manipulator's weight is applied at its CM. If the only other force applied to the manipulator is the force at its base, $-\mathbf{f}_B$, then the following equation holds

$$-\mathbf{f}_B + M\mathbf{g} = \mathbf{f}_{ext} = \frac{d}{dt}\{M\dot{\mathbf{r}}_{CM}\} \quad (1)$$

where M is the total manipulator mass, \mathbf{g} is the acceleration of gravity vector, and $\dot{\mathbf{r}}_{CM}$ is the velocity of the system CM. Therefore, the force transmitted to the base is given by

$$\mathbf{f}_B = -\frac{d}{dt}\{M\dot{\mathbf{r}}_{CM}\} + M\mathbf{g} \quad (2)$$

and has a dynamic component due to the change in system's linear momentum, and a static component due to gravity (which is zero in space). The concern here is to eliminate the dynamic component of base force reactions, since they are partly responsible for base excitation. The dynamic components in Eq. (2) are zero if the system CM does not accelerate, i.e. if $\dot{\mathbf{r}}_{CM} = \text{const.}$ Assuming zero initial CM velocity, integration of this condition yields $\mathbf{r}_{CM} = \text{const.}$, in other words, to transmit zero dynamic forces, the manipulator's CM has to be fixed. In principle, this condition can be achieved by design. To this end, note that by definition

$$\mathbf{r}_{CM} = \frac{1}{M} \sum_{j=1}^l m_j \mathbf{r}_{c,j} \quad (3)$$

where l is the number of manipulator links, m_j is the mass of the j^{th} link and $\mathbf{r}_{c,j}$ the position vector of its CM. Differentiating Eq. (3) and using the chain rule, results in

$$(4)$$

where, by definition

$$= \sum_{j=1}^l m_j \frac{\partial \mathbf{r}_{c,j}}{\partial q_i} \quad (5)$$

In the above relationship, n is the number of DOF, \dot{q}_i is the i^{th} joint rate, \mathbf{J} is a matrix whose columns are the $\frac{\partial \mathbf{r}_{c,j}}{\partial q_i}$ vectors, and $\dot{\mathbf{q}}$ is the vector of joint rates. Note that from Eq.(4) the condition $\dot{\mathbf{r}}_{CM} = \text{constant}$, can hold for any set of $\dot{\mathbf{q}}$ if and only if all $\frac{\partial \mathbf{r}_{c,j}}{\partial q_i}$ are identically equal to zero, or equivalently when $\mathbf{J} = \mathbf{0}$. In principle, the n conditions $\frac{\partial \mathbf{r}_{c,j}}{\partial q_i} = 0$ can be satisfied by proper system design, usually by force balancing.

It can be shown that the equations of motion of a manipulator can be written as [13]

$$(6)$$

where $\mathbf{q} = [q_1, \dots, q_n]^T$ is the vector of generalized coordinates, \mathbf{t} the vector of actuator torques, $\mathbf{H}(\mathbf{q})$ is the $n \times n$ manipulator mass matrix, $\mathbf{V}(\mathbf{q}, \dot{\mathbf{q}})$ is the vector of nonlinear velocity terms, and \mathbf{g} is the constant acceleration due to gravity vector. Consequently, setting equal to zero force balances the manipulator and simplifies the system's dynamics. Note that force balancing is not possible for any manipulator; for example, for the case of planar systems without axisymmetric link groupings, force balancing by internal mass redistribution is possible if, and only if, for each link there is a path to the ground by way of revolutes only [8]. Hence, in this paper we consider manipulators with revolute joints, only.

The case of base moment balancing is more complicated. The moment transmitted to the base of the manipulator, \mathbf{n}_B , is given by

$$(7)$$

where \mathbf{I}_j is the j^{th} link inertia, $\dot{\theta}_j$ its inertial angular velocity. It can be recognized that the sum in Eq. (7) represents the angular momentum of the manipulator with respect to its base. The static moment can be eliminated by fixing the system CM at the first joint. Assuming zero initial velocities, Eq. (7) suggests that to eliminate dynamic moment disturbances this angular momentum must be zero

$$(8a)$$

The above expression can be written compactly as

$$\mathbf{D}(\mathbf{q})\dot{\mathbf{q}} = \mathbf{0} \quad (8b)$$

where $\mathbf{D}(\mathbf{q})$ is an inertia-type matrix, of size $3 \times n$ [3]. In general, it not possible to set by design $\mathbf{D} = \mathbf{0}$. Condition (8) can also be achieved by trajectories for which $\dot{\mathbf{q}}$ is in the null space of $\mathbf{D}(\mathbf{q})$. In practice, finding such trajectories is very difficult, because Eq. (8) cannot be integrated to yield constraints in terms of the \mathbf{q} 's. As shown in this paper, finding such trajectories can be simplified by proper design.

Consider next a planar manipulator with revolute joints for which the dynamic reaction forces were eliminated. If s actuators are mounted at the base and act along the same axis \mathbf{k} , then the \mathbf{n}_B is

$$\mathbf{n}_B = -(\tau_1 + \dots + \tau_s)\mathbf{k} = \sum_{i=1}^s \left\{ \sum_{j=1}^n h_{ij} \ddot{q}_j + \sum_{j=1}^n \sum_{k=1}^n \left(\frac{\partial h_{ij}}{\partial q_k} - \frac{1}{2} \frac{\partial h_{jk}}{\partial q_i} \right) \dot{q}_j \dot{q}_k \right\} \mathbf{k} \quad (9)$$

where h_{ij} are the components of the system's mass matrix \mathbf{H} . The condition $\mathbf{n}_B = \mathbf{0}$ results in a very complicated constraint among accelerations, velocities and positions. However, if all h_{ij} are constant, i.e. if the mass matrix is invariant, the above equation becomes a second order linear differential equation which can be integrated twice. The first integration results is Eq. (8b), i.e. the angular momentum of the system, where $\mathbf{D}(\mathbf{q})$ is a constant matrix. Integrating this equation once more results in a constraint between the joint angles; satisfying this constraint generates motions that do not transmit moment reactions to the base. If the manipulator has also been force balanced, then this constraint can be visualized as a *reactionless* path in the joint space. This method is employed in the design of the two reaction-free manipulators presented in this paper.

From the above analysis, the following two design guidelines emerge for reactionless manipulators (a) force balance a manipulator with revolute joints to eliminate dynamic forces, and (b) use mass matrix invariance and special planning techniques to maintain zero angular momentum. Since as explained above, guideline (b) introduces a constraint between the joint angles, redundant manipulator designs must be employed for practical designs.

Note that an alternative method for setting \mathbf{n}_B equal to zero, is to use additional base actuators, like reaction wheels, to cancel any reaction moments. This method has been used in space systems [2,3], and was employed in the design of a high-acceleration minipositioner [1]. However, a limitation of this method is that the additional actuators cannot be used to increase the DOFs of a manipulator. In contrast to this, the method proposed in this paper allows the manipulators to be used either as reaction-free, or as redundant systems.

As shown below, these guidelines are implemented on two 3 DOF redundant planar manipulators, with at least two actuators mounted at their base with the actuators acting along the

same axis but in opposite directions. If a single actuator is mounted at the base joint, then it will be required to apply zero torque during a reactionless trajectory; this design would result in a nonholonomic system behavior and will not be discussed in this paper. To maintain planar operation, the manipulators are assumed to be symmetric with respect to their plane of action.

III. MANIPULATOR DESIGN

The above ideas are demonstrated using two manipulator designs that meet the requirements for reaction-free motion. The first is based on a five bar mechanism with an additional link, see Fig. 2 (a), and is referred to as “Manipulator I.” The second is based on a nine-link parallel mechanism, see Fig. 2 (b), and is referred to as “Manipulator II.”

A. Manipulator I.

Consider the 3 DOF parallel manipulator with five mobile links shown Fig. 2 (a). This manipulator is redundant in terms of the in plane positioning requirements. In this section it is shown how a combination of its physical parameters, along with proper trajectory planning, can result in a reactionless manipulator.

As depicted in Fig. 2, the manipulator is composed of a five-bar mechanism (links 1, 2, 3, and 4), connected to an additional link (link 5). The actuators for links 1 and 2 are located at the base, and share a common axis. Therefore, the base moment for this manipulator is given by

$$\mathbf{n}_B = -(\tau_1 + \tau_2)\mathbf{k} \quad (10)$$

where τ_i are actuator torques, and \mathbf{k} is the unit vector normal to the plane of motion. It can be seen that for $\mathbf{n}_B = \mathbf{0}$, the two base actuators must apply equal and opposite torques to the base. This requires special trajectories, and therefore, when operating under the zero reaction mode, the manipulator will have two DOF.

For this manipulator, detailed expressions for $\mathbf{H}(\mathbf{q})$, $\mathbf{V}(\mathbf{q}, \dot{\mathbf{q}})$, $\mathbf{G}(\mathbf{q})$, and $\mathbf{D}(\mathbf{q})$, are provided in Appendix A. The requirements for force balancing are derived by setting Equations (A4)

equal to zero. For zero moment transmission, either $\mathbf{H}(\mathbf{q})$ or $\mathbf{D}(\mathbf{q})$ must become independent of the configuration \mathbf{q} . This is achieved by setting configuration dependent terms equal to zero. Both zero dynamic force and moment transmission is possible when the following four conditions hold

$$l_{c5} = 0 \quad (11a)$$

$$m_1 l_{c1} + m_3 l_{c3} + m_4 l_1 + m_5 l_1 = 0 \quad (11b)$$

$$m_2 l_{c2} + m_3 l_2 - m_4 l_{c4} - m_5 l_4 = 0 \quad (11c)$$

$$m_3 l_2 l_{c3} - m_4 l_1 l_{c4} - m_5 l_1 l_4 = 0 \quad (11d)$$

where l_{ci} is the CM of link i . Although Eq. (11a) is trivial, the last three equations correspond to four unknowns, namely to l_{ci} for $i=1, \dots, 4$. Eqs. (11b-d) are written in matrix form as

$$\begin{bmatrix} m_1 & 0 & m_3 & 0 \\ 0 & m_2 & 0 & -m_4 \\ 0 & 0 & m_3 \frac{l_2}{l_1} & -m_4 \end{bmatrix} \begin{bmatrix} l_{c1} \\ l_{c2} \\ l_{c3} \\ l_{c4} \end{bmatrix} = \begin{bmatrix} m_5 l_4 \\ -(m_4 + m_5) l_1 \\ m_5 l_4 - m_3 l_2 \end{bmatrix} \quad (12)$$

or compactly as

$$\mathbf{A} \mathbf{l}_c = \mathbf{k} \quad (13)$$

This linear system is under-constrained and has an infinite number of solutions including the minimum-norm solution. If not all l_{ci} have the same importance in terms of feasible designs, one can minimize $\mathbf{W} \mathbf{l}_c$ instead of \mathbf{l}_c , where \mathbf{W} is a diagonal weighting matrix. In such case, the weighted minimum norm solution for \mathbf{l}_c is

$$\mathbf{l}_c = \boxed{\mathbf{V} \mathbf{A}^T (\mathbf{A} \mathbf{V} \mathbf{A}^T)^{-1}} \mathbf{k} \quad (14a)$$

where

$$\mathbf{V} = \mathbf{W}^{-1} (\mathbf{W}^{-1})^T \quad (14b)$$

Eq. (13) was solved for given mass and geometric manipulator properties, and for $\mathbf{W} = \text{diag}(0.14, 0.2, 1.0, 1.0)$. The results are displayed in Table I. The above parameters result in an invariant mass matrix along with a force balanced manipulator. The dynamic equations reduce to

$$\begin{bmatrix} \tau_1 \\ \tau_2 \\ \tau_3 \end{bmatrix} = \begin{bmatrix} h_{11} & 0 & 0 \\ 0 & h_{22} & h_{23} \\ 0 & h_{32} & h_{33} \end{bmatrix} \begin{bmatrix} \ddot{q}_1 \\ \ddot{q}_2 \\ \ddot{q}_3 \end{bmatrix} \quad (15)$$

B. Manipulator II

Here we briefly present the design for a manipulator with nine mobile links and all its three actuators mounted at its base. This manipulator is redundant in terms of the in plane positioning requirements, and was proposed as a finger for a mechanical hand [12]. As depicted in Fig. 2 (b), the manipulator is composed of three parallel mechanisms; links 1-4-6 are always mutually parallel, and so are 2-5-8 and 3-7-9. Each set of parallel links can be made to rotate while the other links are either stationary or translating. The driving links (1, 2, & 3) and their direct drive actuators are on the base; this characteristic simplifies the decoupling of the manipulator's mass matrix and results in simpler dynamic equations. As evident from Fig. 2 (b), the following sets of links share common lengths: $l_1 = l_4 = l_6$, $l_5 = l_8$, and $l_3 = l_7$.

Since all three joint actuators share the same axis, the total moment applied to the base is

$$\mathbf{n}_B = -(\tau_1 + \tau_2 + \tau_3)\mathbf{k} \quad (16)$$

The same procedure as described above is applied to this manipulator. To this end, detailed expressions for $\mathbf{H}(\mathbf{q})$, $\mathbf{V}(\mathbf{q}, \dot{\mathbf{q}})$, and $\mathbf{D}(\mathbf{q})$, are provided in Appendix A. Setting to zero results in three equations, and eliminating configuration dependent terms in $\mathbf{D}(\mathbf{q})$ or $\mathbf{H}(\mathbf{q})$, yields three more [14]. As for the previous manipulator, these equations have the form of Eq. (13). In this case, there are nine design parameters, namely the locations of the nine centers of mass, l_{c_i} , $i=1, \dots, 9$ and the problem be expressed in matrix format as follows

$$\begin{bmatrix} m_1 & 0 & 0 & m_4 & 0 & m_6 & 0 & 0 & 0 \\ 0 & m_2 & 0 & 0 & -m_5 & 0 & 0 & -m_8 & 0 \\ 0 & 0 & m_3 & 0 & 0 & 0 & m_7 & 0 & -m_9 \\ 0 & 0 & 0 & m_4 \frac{l_2}{l_1} & -m_5 & 0 & 0 & -m_8 & 0 \\ 0 & 0 & 0 & 0 & 0 & m_6 \frac{l_3}{l_1} & m_7 & 0 & -m_9 \\ 0 & 0 & 0 & 0 & 0 & 0 & 0 & -m_8 \frac{l_3}{l_5} & m_9 \end{bmatrix} \begin{bmatrix} l_{c1} \\ l_{c2} \\ l_{c3} \\ l_{c4} \\ l_{c5} \\ l_{c6} \\ l_{c7} \\ l_{c8} \\ l_{c9} \end{bmatrix} = \begin{bmatrix} -(m_5 + m_7 + m_8 + m_9)l_1 \\ m_9l_5 - m_4l_2 \\ -(m_8 + m_6)l_3 \\ m_9l_5 \\ -m_8l_3 \\ 0 \end{bmatrix} \quad (17)$$

Again a minimum norm solution is sought. Using $\mathbf{W} = \text{diag}(1.0, 0.2, 1.0, 1.2, 1.0, 1.0, 1.0, 1.0, 1.0)$, Eqs. (14) are solved and the manipulator's geometric parameters of the manipulator are displayed in Table II. Then, the dynamic equations given by Eq. (6) become

$$\begin{bmatrix} \tau_1 \\ \tau_2 \\ \tau_3 \end{bmatrix} = \begin{bmatrix} h_{11} & 0 & 0 \\ 0 & h_{22} & 0 \\ 0 & 0 & h_{33} \end{bmatrix} \begin{bmatrix} \ddot{q}_1 \\ \ddot{q}_2 \\ \ddot{q}_3 \end{bmatrix} \quad (18)$$

resulting in a dynamically decoupled system.

IV. REACTIONLESS TRAJECTORY PLANNING

For both manipulators, setting $\mathbf{n}_B = \mathbf{0}$, and using Eqs. (10) & (15) or Eqs. (16) & (18), results in constraints of the form:

$$\ddot{q}_1 + \lambda_2 \ddot{q}_2 + \lambda_3 \ddot{q}_3 = 0 \quad (19)$$

where λ_1 , λ_2 , and λ_3 are constants and functions of the invariant mass matrix elements. Eq. (19) is integrated to yield a constraint in terms of the link angles \mathbf{q} . With zero initial conditions for the rates, the integration results in

$$\dot{q}_1 + \lambda_2 \dot{q}_2 + \lambda_3 \dot{q}_3 = 0 \quad (20)$$

which is a manifestation of zero angular momentum, see Eq. (8). Physically, this equation suggests that reactionless motions require that at least one joint be moving opposite to some other one. Since λ_2 and λ_3 are constants, the equation can be integrated again to yield

$$q_1 + \lambda_2 q_2 + \lambda_3 q_3 = b \quad (21)$$

where the constant b is called here the *pose constant*, because it depends on the initial set of link angles. Equation (21) represents a *plane* in the space of $q_1 - q_2 - q_3$, with $\mathbf{n} = [1, \lambda_2, \lambda_3]^T$ its normal vector. Moving in a reactionless path requires Eq. (21) to be satisfied. Furthermore, for a given initial configuration \mathbf{q} , the pose constant is set, and all via points and the target must be on the same plane in the \mathbf{q} space. Since a redundant manipulator can reach points in its workspace in more than one pose, it follows from Eq. (21) that a single x-y coordinate can have a range of b constants associated with it. Each of these b constants defines a different plane, but since the normal vector \mathbf{n} is fixed for a given manipulator, all these planes are parallel.

Given a point in the x-y plane, the range of pose constants which correspond to it can be found using inverse kinematic relationships. A plot of q_1 for each pose versus the pose constant b is shown in Fig. 3, for two (x, y) points. This plot can also be used to determine if two points can be joined by a reactionless path. To this end, it suffices to have plot overlap, such as the one shown in Fig. 3. For example, the point $(0.55, 0.0)$ is reachable from $(0.8, 0.0)$ if the initial angle q_1 is between 0.50 and 1.25 rad.

Path planning can be facilitated if the set of points that can be accessed by a reactionless path from some initial configuration is known. To find this *reactionless workspace*, it is assumed that the first joint q_1 can rotate freely, while the relative joint angles a_1 , and a_2 defined in Fig. 2, comply with some given joint limits.

Using manipulator II as an example, Fig. 2 (b), yields the following expressions for a_1 and a_2

$$a_1 = q_2 - q_1 \quad (22a)$$

$$a_2 = q_3 - q_2 + \pi \quad (22b)$$

The forward kinematic equations for this manipulator are, see Fig. 2 (b)

$$x = l_1 \cos(q_1) - l_5 \cos(q_2) - l_9 \cos(q_3) \quad (23a)$$

$$y = l_1 \sin(q_1) - l_5 \sin(q_2) - l_9 \sin(q_3) \quad (23b)$$

Substituting Eq. (22) in Eqs. (23), and writing the result in matrix form, results in

$$\begin{bmatrix} x \\ y \end{bmatrix} = \begin{bmatrix} \cos(q_1) & -\sin(q_1) \\ \sin(q_1) & \cos(q_1) \end{bmatrix} \begin{bmatrix} l_1 - l_5 \cos(a_1) + l_9 \cos(a_1 + a_2) \\ -l_5 \sin(a_1) + l_9 \sin(a_1 + a_2) \end{bmatrix} \quad (24)$$

Furthermore, using Eqs. (21) and (22), q_1 can be expressed as

$$q_1 = \frac{b}{1 + \lambda_2 + \lambda_3} + \frac{\lambda_3(\pi - a_2) - a_1(\lambda_2 + \lambda_3)}{1 + \lambda_2 + \lambda_3} = b^* + \phi(a_1, a_2) \quad (25)$$

where $b^* = b/(1 + \lambda_2 + \lambda_3)$ is a constant, and ϕ an angle function of a_1 and a_2 . Substituting Eq. (25) in Eq. (24) yields

$$\begin{bmatrix} x \\ y \end{bmatrix} = \begin{bmatrix} c(b^*) & -s(b^*) \\ s(b^*) & c(b^*) \end{bmatrix} \begin{bmatrix} c(\phi) & -s(\phi) \\ s(\phi) & c(\phi) \end{bmatrix} \begin{bmatrix} l_1 - l_5 c(a_1) + l_9 c(a_1 + a_2) \\ -l_5 s(a_1) + l_9 s(a_1 + a_2) \end{bmatrix} \quad (26)$$

where $c()$, $s()$ denote the cosine and the sin of an angle. For a given initial pose, b and therefore b^* , are fixed. Hence, all the points that can be accessed starting from an initial pose can be found by varying the relative joint angles in the allowed range. Similar equations apply to manipulator I.

The reactionless workspace is plotted in the Cartesian plane using Eq. (26) above. The resulting workspaces for manipulators I and II are shown in Fig. 4 for some initial pose constant b . Any two points in these workspace, shown as the gray region, can be connected by a reactionless path. Note that since the pose constant only appears in the first rotation matrix in Eq. (26), the *shape* of the reactionless workspace is independent of this constant. However, its *orientation* on the Cartesian plane depends on it, i.e. changing the pose constant has the effect of rotating the gray area shown in Fig. 4.

V. SIMULATIONS AND COMPARISONS

The dynamic equations of the 3 DOF parallel manipulators were programmed into MATLAB. The linear system of Eqs. (12) and (17) were used to compute the physical parameters of the manipulators, required for reactionless motions. The results are displayed in Tables I and II.

To calculate the reaction moments at the base, an initial and final point were chosen from the reactionless region and the travel time was set at 1.5 s. The x - y pairs along with the b constant determine the initial and final angles of the manipulator, \mathbf{q}_A , and \mathbf{q}_B , see Eqs. (22), (25) and (26). The reactionless paths selected are straight line in the three-dimensional joint space connecting \mathbf{q}_A , and \mathbf{q}_B , since such lines lie on the plane defined by Eq. (21). In all simulation results, the manipulators transmit zero reaction forces to their bases.

Quintic polynomial trajectories were used in the simulation in order to have continuous joint velocity and acceleration profiles. A computed torque control scheme was employed to determine the motor torques required, and the control gains were kept the same in all cases. Fig. 5 shows snapshots of a reactionless motion sequence in Cartesian space for manipulator I. It can be noticed that as the distal link moves outwards, the first link moves in opposite way, so that the angular momentum of the system is conserved. Fig. 5 also includes the required actuator torques τ_1 , τ_2 , and τ_3 , during the reactionless motion. Note that the resulting base reaction is practically zero.

Fig. 6a depicts the required actuator torques τ_1 , τ_2 , and τ_3 , as well as the resultant base reaction for a manipulator II reactionless trajectory. As shown in Fig. 6 (a), This reaction is practically zero. For comparison, manipulator II was simulated to follow the same Cartesian path as in Fig. 6 (a), but with different poses at the via points; thus in the second motion no reactionless plane was adhered to. As can be seen from Fig. 6 (b), in this case base reactions are substantial. Fig. 6 also includes snapshots of the corresponding motion sequences in Cartesian space. From the snapshots it is evident that while some links move opposite to other links in the reactionless motion, this does not occur in the other case.

VI. CONCLUSIONS

Analysis of force transmission properties of manipulators has shown that dynamic reactions can be eliminated if the system CM is kept fixed. For planar mechanisms with revolute joints, this condition can be satisfied by proper design. However, moment balancing of such systems requires in general appropriate trajectory planning. It was shown that rendering the manipulator mass matrix invariant, simplifies the planning of reactionless paths, by requiring that these paths belong in fixed orientation joint space planes. Motions planned in such a way result in minimal reactions, whereas non-reactionless motions transmit large reactions. Two three-DOF planar manipulators were designed according to the analysis in this paper, and were used to demonstrate the value of the proposed methods. An additional advantage of these methods is that the manipulators can be used either as redundant, or as two DOF reactionless systems.

VII. ACKNOWLEDGMENTS

The support of this work by the Fonds pour la Formation de Chercheurs et l'Aide a la Recherche (FCAR), and by the Natural Sciences and Engineering Council of Canada (NSERC) is gratefully acknowledged.

REFERENCES

- [1] Karidis, J.P., et al, "The Hummingbird Minipositioner - Providing Three Axis Motion at 50 G's With Low Reactions," *Proc. 1992 IEEE Conf. Robotics and Automation*, Nice, France, May 1992.
- [2] Dubowsky, S. and Torres, M.A., "Path Planning for Space Manipulators to Minimize Spacecraft Attitude Disturbance," *Proc.1991 IEEE Conf. Robotics and Automation*, Sacramento, CA, April 1991.

- [3] Papadopoulos, E. and Dubowsky, S., "On the Nature of Control Algorithms for Free-floating Space Manipulators," *IEEE Trans. on Robotics and Automation*, Vol. 7, No. 6, Dec. 1991, pp. 750-758.
- [4] Rohn, D., et al, "Microgravity Robotics Technology Program," *ISA/88 Int. Conf.*, Houston, TX, 1988.
- [5] Erb, B., "Canada's Mobile Servicing System," *Space Technology*, Vol. 10, No 1/2, pp. 19-25, 1990.
- [6] West, H., et al. "Experimental Simulation of Manipulator Base Compliance," in *Experimental Robotics I*, V. Hayward, and O. Khatib (Eds.), Lect. Notes in Control and Information Sciences #139, Springer Verlag, 1990.
- [7] Quinn, R.D., et al., "Redundant Manipulators for Momentum Compensation in a Micro-Gravity Environment," *AIAA Guidance, Navigation, and Control Conf.*, Minneapolis, MN, August 15-17, 1988.
- [8] Berkof, R.S., et al., "Balancing of Linkages," *Shock and Vibration Digest.*, 9, No.6, pp. 3-10, 1977.
- [9] Walker, M.J. and Oldham, K., "General Theory of Force Balancing Using Counterweights," *Mechanism and Machine Theory*, 13, pp. 175-185, 1978.
- [10] Kazerooni, H., "Design and Analysis of the Statically Balanced Direct-Drive Robot Manipulator," *Robotics and CIM*, 6, no.4, pp. 287-293, 1989.
- [11] Kaufman, R.E. and Sandor, G.N., "Complete Force Balancing of Spatial Linkages," *ASME J. of Engineering for Industry*, pp. 620-626, 1971.
- [12] Youcef-Toumi, K. and Yahiaoui, M., "The Design of a Mini Direct-Drive Finger With Decoupled Dynamics," *ASME 1988 WAM*, pp. 411-415.
- [13] Abu-Abed, A., "Analysis and Design of Planar Zero Reaction Robots," *Center for Intelligent Machines Internal Report CIM 93-24*, McGill University, Montreal, 1993.

- [14] Papadopoulos, E. and Abu-Abed, A., “Design and Motion Planning for a Zero-Reaction Manipulator,” *Proc. of the IEEE Int. Conf. on Robotics and Automation*, San Diego, CA, May 1994, pp. 1554-1559.

APPENDIX A

For the 3 DOF manipulator in Fig. 2 (a), the equations of motion have the form given by Eq.

(6). The components of the mass matrix \mathbf{H} are given by

$$\begin{aligned}
 h_{11} &= I_1 + I_3 + m_1 l_{c1}^2 + m_3 l_{c3}^2 + m_4 l_1^2 + m_5 l_1^2 \\
 h_{12} &= (m_3 l_2 l_{c3} - m_4 l_1 l_{c4} - m_5 l_1 l_4) \cos(q_1 - q_2) - m_5 l_1 l_{c5} \cos(q_1 - q_2 - q_3) \\
 h_{13} &= -m_5 l_1 l_{c5} \cos(q_1 - q_2 - q_3) \\
 h_{22} &= I_2 + I_4 + I_5 + m_2 l_{c2}^2 + m_3 l_2^2 + m_4 l_{c4}^2 + m_5 l_{c5}^2 + m_5 l_4^2 + 2m_5 l_4 l_{c5} \cos(q_3) \\
 h_{23} &= I_5 + m_5 l_{c5}^2 + m_5 l_4 l_{c5} \cos(q_3) \\
 h_{33} &= I_5 + m_5 l_{c5}^2
 \end{aligned} \tag{A1}$$

The components of the \mathbf{V} and $\mathbf{G} = \mathbf{T}\mathbf{g}$ vectors in Eq. (6) are

$$\begin{aligned}
 v_1 &= (m_3 l_2 l_{c3} - m_4 l_1 l_{c4} - m_5 l_1 l_4) \sin(q_1 - q_2) \dot{q}_2^2 \\
 &\quad - m_5 l_1 l_{c5} \sin(q_1 - q_2 - q_3) (\dot{q}_2 + \dot{q}_3) \\
 v_2 &= (-m_3 l_2 l_{c3} + m_4 l_1 l_{c4} + m_5 l_1 l_4) \sin(q_1 - q_2) \dot{q}_1^2 \\
 &\quad + m_5 l_1 l_{c5} \sin(q_1 - q_2 - q_3) \dot{q}_1^2 \\
 &\quad - 2m_5 l_4 l_{c5} \sin(q_3) \dot{q}_2 \dot{q}_3 - m_5 l_4 l_{c5} \sin(q_3) \dot{q}_3^2 \\
 v_3 &= m_5 l_{c5} l_1 \sin(q_1 - q_2 - q_3) \dot{q}_1^2 - m_5 l_{c5} l_4 \sin(q_3) \dot{q}_2^2 \\
 g_1 &= (m_1 l_{c1} + m_3 l_{c3} + m_4 l_1 + m_5 l_1) g \cos(q_1) \\
 g_2 &= (m_2 l_{c2} + m_3 l_2 - m_4 l_{c4} - m_5 l_4) g \cos(q_2) - m_5 l_{c5} g \cos(q_2 + q_3)
 \end{aligned}$$

$$g_3 = -m_5 l_{c5} g \cos(q_2 + q_3) \quad (\text{A3})$$

The columns of the matrix given by Eq. (5) are

$$(\text{A4})$$

where the vectors are given by

$$(k = 1,2) \quad (\text{A5})$$

The inertia-type matrix $\mathbf{D}(\mathbf{q})$ is given by

$$\mathbf{D}(\mathbf{q}) = [d_1, d_2, d_3] \quad (\text{A6})$$

with elements given by

$$\begin{aligned} d_1 &= I_1 + I_3 + m_1 l_{c1}^2 + m_3 l_{c3}^2 + m_4 l_1^2 + m_5 l_1^2 + \\ &\quad + (m_3 l_2 l_{c3} - m_4 l_1 l_{c4} - m_5 l_1 l_4) \cos(q_1 - q_2) \\ &\quad - m_5 l_1 l_{c5} \cos(q_1 - q_2 - q_3) \\ d_2 &= I_2 + I_4 + I_5 + m_2 l_{c2}^2 + m_3 l_2^2 + m_4 l_{c4}^2 + m_5 l_{c5}^2 + m_5 l_4^2 + 2m_5 l_4 l_{c5} \cos(q_3) + \\ &\quad + (m_3 l_2 l_{c3} - m_4 l_1 l_{c4} - m_5 l_1 l_4) \cos(q_1 - q_2) \\ &\quad - m_5 l_1 l_{c5} \cos(q_1 - q_2 - q_3) \\ d_3 &= I_5 + m_3 l_{c5}^2 - m_5 l_1 l_{c5} \cos(q_1 - q_2 - q_3) \end{aligned} \quad (\text{A7})$$

For the 3 DOF manipulator in Fig. 2 (b), the equations of motion also have the form given by Eq. (6). The components of the mass matrix \mathbf{H} are given by

$$\begin{aligned} h_{11} &= I_1 + I_4 + I_6 + m_1 l_{c1}^2 + m_4 l_{c4}^2 + m_6 l_{c6}^2 + (m_5 + m_7 + m_8 + m_9) l_1^2 \\ h_{12} &= (m_4 l_2 l_{c4} - m_5 l_1 l_{c5} - m_8 l_1 l_{c8} - m_9 l_1 l_5) \cos(q_1 - q_2) \\ h_{13} &= (m_6 l_3 l_{c6} + m_7 l_1 l_{c7} + m_8 l_1 l_7 - m_9 l_1 l_{c9}) \cos(q_1 - q_3) \end{aligned}$$

$$\begin{aligned}
h_{22} &= I_2 + I_5 + I_8 + m_2 l_{c2}^2 + m_5 l_{c5}^2 + m_8 l_{c8}^2 + m_4 l_2^2 + m_9 l_5^2 \\
h_{23} &= (m_9 l_5 l_{c9} - m_8 l_7 l_{c8}) \cos(q_2 - q_3) \\
h_{33} &= I_3 + I_7 + I_9 + m_3 l_{c3}^2 + m_7 l_{c7}^2 + m_9 l_{c9}^2 + m_6 l_3^2 + m_8 l_7^2
\end{aligned} \tag{A8}$$

The components of the \mathbf{V} and $\mathbf{G} = {}^T \mathbf{g}$ vectors in Eq. (6) are

$$\begin{aligned}
v_1 &= (m_4 l_2 l_{c4} - m_5 l_1 l_{c5} - m_8 l_1 l_{c8} - m_9 l_1 l_5) \sin(q_1 - q_2) \dot{q}_2^2 \\
&\quad + (m_6 l_3 l_{c6} + m_7 l_1 l_{c7} + m_8 l_1 l_7 - m_9 l_1 l_{c9}) \sin(q_1 - q_3) \dot{q}_3^2 \\
v_2 &= (-m_4 l_2 l_{c4} + m_5 l_1 l_{c5} + m_8 l_1 l_{c8} + m_9 l_1 l_5) \sin(q_1 - q_2) \dot{q}_1^2 \\
&\quad - (m_8 l_7 l_{c8} + m_9 l_5 l_{c9}) \sin(q_2 - q_3) \dot{q}_3^2 \\
v_3 &= (-m_6 l_3 l_{c6} - m_7 l_1 l_{c7} - m_8 l_1 l_7 + m_9 l_1 l_{c9}) \sin(q_1 - q_3) \dot{q}_1^2 \\
&\quad + (m_8 l_7 l_{c8} - m_9 l_5 l_{c9}) \sin(q_2 - q_3) \dot{q}_2^2
\end{aligned} \tag{A9}$$

$$\begin{aligned}
g_1 &= (m_1 l_{c1} + m_4 l_{c4} + m_6 l_{c6} + (m_5 + m_7 + m_8 + m_9) l_1) g \cos(q_1) \\
g_2 &= (m_2 l_{c2} + m_4 l_2 - m_5 l_{c5} - m_8 l_{c8} - m_9 l_5) g \cos(q_2) \\
g_3 &= (m_3 l_{c3} + m_6 l_3 + m_7 l_{c7} + m_8 l_7 - m_9 l_{c9}) g \cos(q_3)
\end{aligned} \tag{A10}$$

The columns of the matrix given by Eq. (5) are

$$\begin{aligned}
&1 \\
&2 \\
&3
\end{aligned} \tag{A11}$$

where k , ($k = 1, 2, 3$), are given by

$$\tag{A12}$$

The elements of the inertia-type matrix $\mathbf{D}(\mathbf{q})$, see also Eq. (A6) are given by

$$\begin{aligned}
d_1 &= I_1 + I_4 + I_6 + m_1 l_{c1}^2 + m_4 l_{c4}^2 + m_6 l_{c6}^2 + (m_5 + m_7 + m_8 + m_9) l_1^2 + \\
&\quad + (m_4 l_2 l_{c4} - m_5 l_1 l_{c5} - m_8 l_1 l_{c8} - m_9 l_1 l_5) \cos(q_1 - q_2) + \\
&\quad + (m_6 l_3 l_{c6} + m_7 l_1 l_{c7} + m_8 l_1 l_7 - m_9 l_1 l_{c9}) \cos(q_1 - q_3) \\
d_2 &= I_2 + I_5 + I_8 + m_2 l_{c2}^2 + m_5 l_{c5}^2 + m_8 l_{c8}^2 + m_4 l_2^2 + m_9 l_5^2 + \\
&\quad + (m_4 l_2 l_{c4} - m_5 l_1 l_{c5} - m_8 l_1 l_{c8} - m_9 l_1 l_5) \cos(q_1 - q_2) \\
&\quad + (m_9 l_5 l_{c9} - m_8 l_7 l_{c8}) \cos(q_2 - q_3) \\
d_3 &= I_3 + I_7 + I_9 + m_3 l_{c3}^2 + m_7 l_{c7}^2 + m_9 l_{c9}^2 + m_6 l_3^2 + m_8 l_7^2 + \\
&\quad + (m_6 l_3 l_{c6} + m_7 l_1 l_{c7} + m_8 l_1 l_7 - m_9 l_1 l_{c9}) \cos(q_1 - q_3) \\
&\quad + (m_9 l_5 l_{c9} - m_8 l_7 l_{c8}) \cos(q_2 - q_3)
\end{aligned} \tag{A13}$$

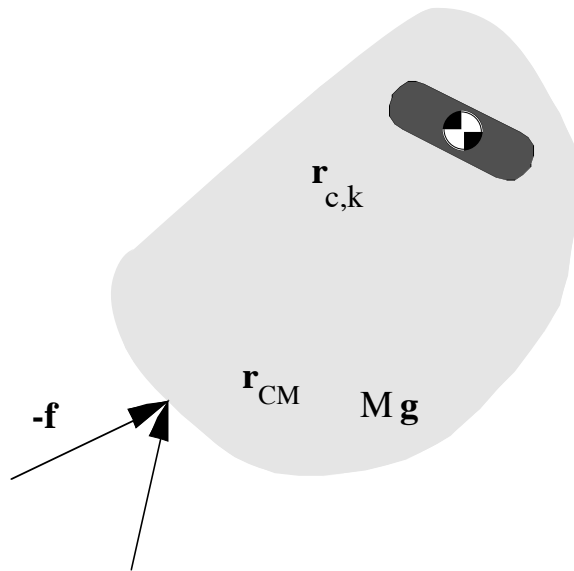
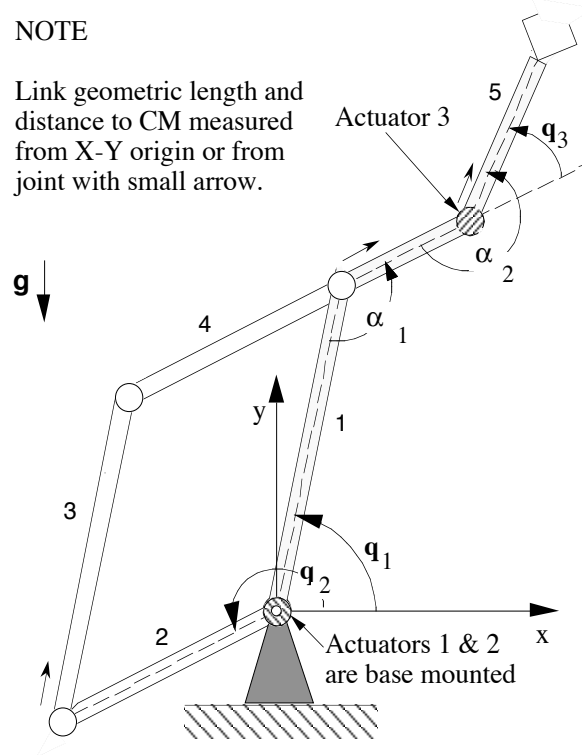


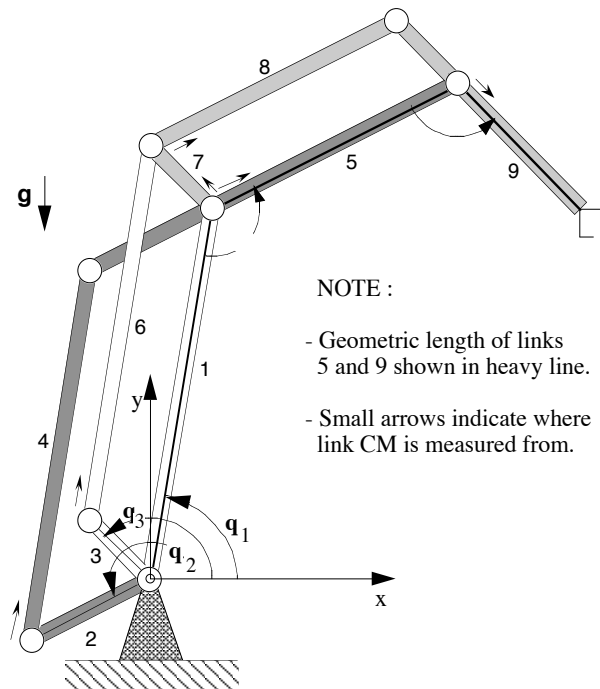
Fig. 1. Forces and moments applied on manipulator.

NOTE

Link geometric length and distance to CM measured from X-Y origin or from joint with small arrow.



(a)



(b)

Fig. 2. Two 3 DOF manipulators. (a) A five-bar mechanism manipulator with an additional link, (b) a nine-link parallel manipulator.

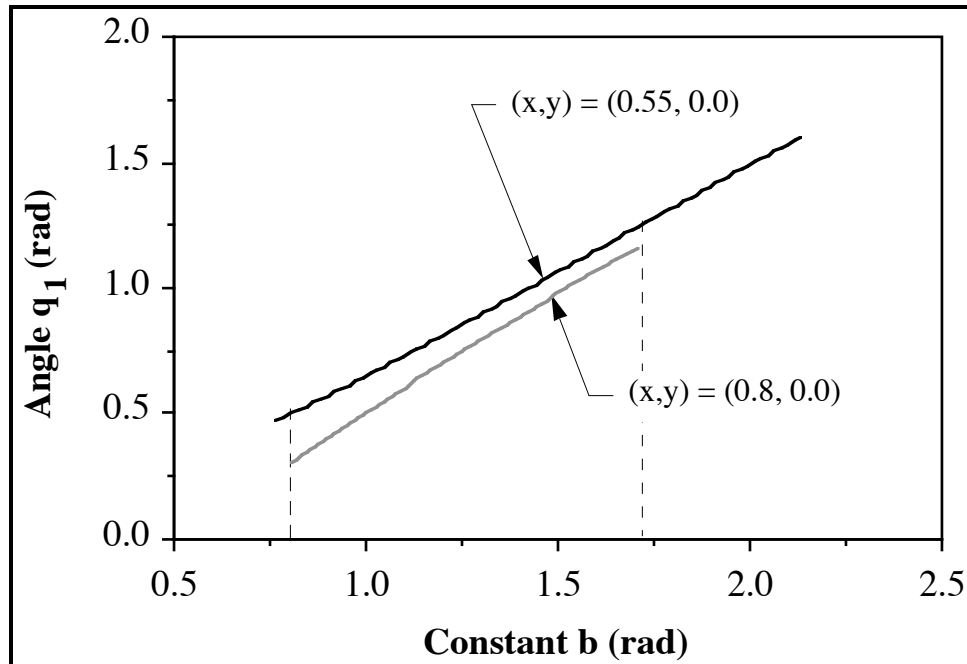
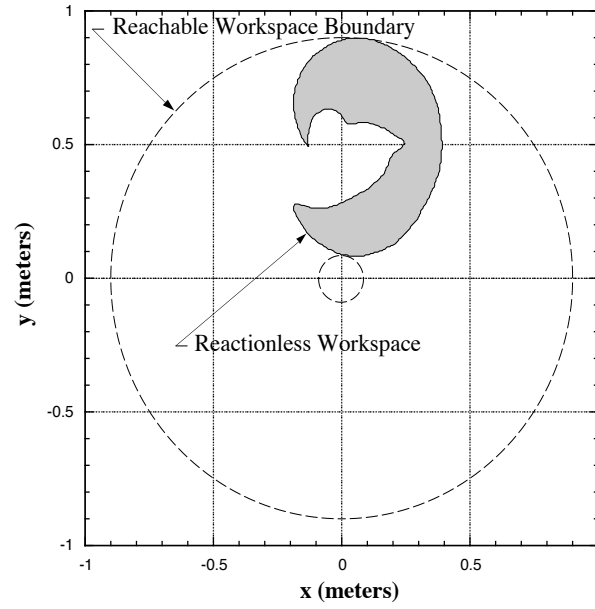
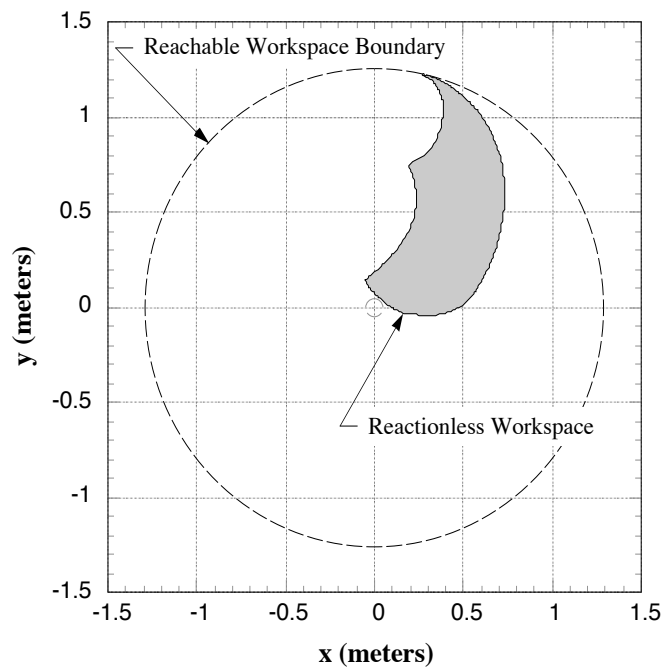


Fig. 3. Range of q_1 and corresponding b pose constants for two (x, y) points



(a)



(b)

Fig. 4. Reactionless workspaces. (a) Manipulator I for $b = 2.2$ rad, (b) Manipulator II for $b = 2.4$ rad.

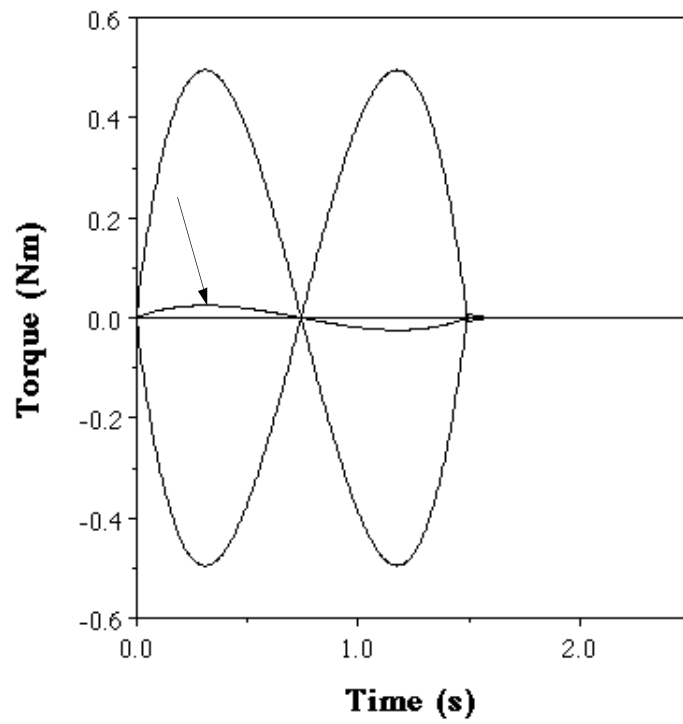
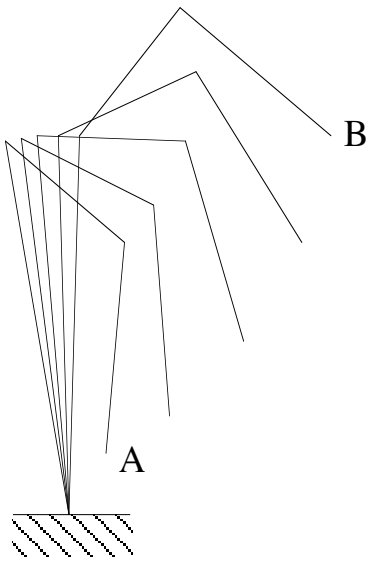
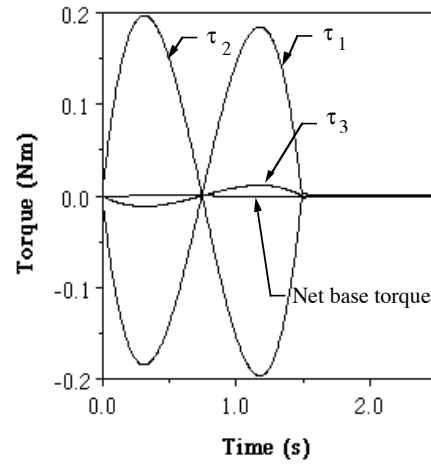
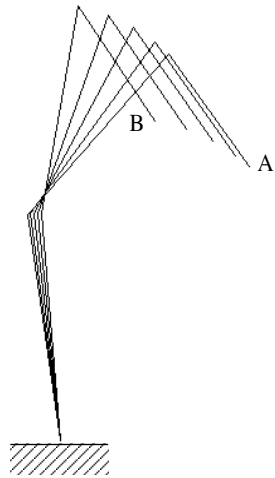
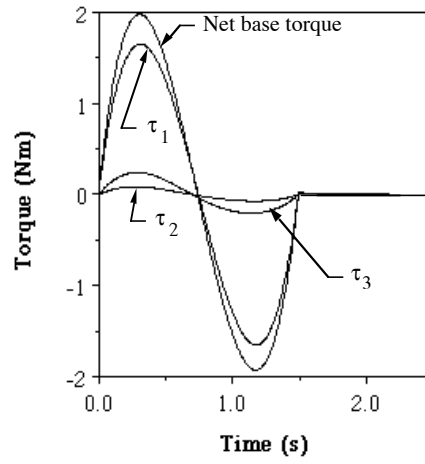
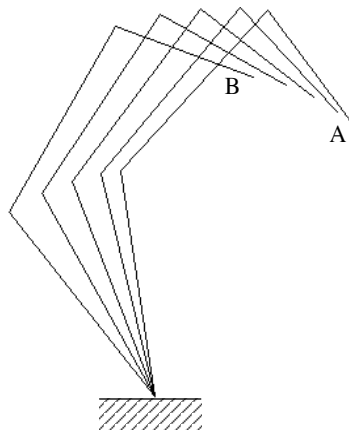


Fig. 5. Reactionless Cartesian motion and torque profiles for Manipulator I.



(a)



(b)

Fig. 6 Cartesian motions and resulting torque profiles for Manipulator II. (a) Reactionless, (b) Cartesian path as in (a), but non-reactionless.

List of Figures

- Fig. 1. Forces and moments applied on manipulator.
- Fig. 2. Two 3 DOF manipulators. (a) A five-bar mechanism manipulator with an additional link, (b) a nine-link parallel manipulator.
- Fig. 3. Range of q_1 and corresponding b pose constants for two (x, y) points
- Fig. 4. Reactionless workspaces. (a) Manipulator I for $b = 2.2$ rad,
(b) Manipulator II for $b = 2.4$ rad.
- Fig. 5. Reactionless Cartesian motion and torque profiles for Manipulator I.
- Fig. 6. Cartesian motions and resulting torque profiles for Manipulator II. (a) Reactionless,
(b) Cartesian path as in (a), but non-reactionless.

Tables

Table I. Manipulator I Parameters

i	l_i (m)	m_i (kg)	I_i (kgm ²)	l_{ci} (m)
1	0.45	4.00	0.1351	-0.2539
2	0.30	0.85	0.0028	-0.1387
3	0.45	0.45	0.0180	0.0571
4	0.20	1.50	0.0245	-0.0819
5	0.25	0.70	0.0093	0

Table II. Manipulator II Parameters

i	l_i (m)	m_i (kg)	I_i (kgm ²)	l_{ci} (m)
1	0.50	7.00	0.2501	-0.2214
2	0.18	1.45	0.0025	-0.1111
3	0.20	2.00	0.0180	-0.1605
4	0.50	1.50	0.0199	0.2016
5	0.46	0.70	0.0215	-0.0110
6	0.50	1.50	0.0419	-0.0349
7	0.20	1.15	0.0143	-0.0682
8	0.46	0.50	0.0162	0.0032
9	0.30	0.25	0.0058	0.0027